



CHORUS

This is the accepted manuscript made available via CHORUS. The article has been published as:

Electroweak phase transition, Higgs diphoton rate, and new heavy fermions

Hooman Davoudiasl, Ian Lewis, and Eduardo Pontón

Phys. Rev. D **87**, 093001 — Published 2 May 2013

DOI: [10.1103/PhysRevD.87.093001](https://doi.org/10.1103/PhysRevD.87.093001)

Electroweak Phase Transition, Higgs Diphoton Rate, and New Heavy Fermions

Hooman Davoudiasl,¹ Ian Lewis,¹ and Eduardo Pontón^{2,1}

¹*Department of Physics, Brookhaven National Laboratory, Upton, NY 11973, USA*

²*Department of Physics, Columbia University, New York, NY 10027, USA*

We show that weak scale vector-like fermions with order one couplings to the Higgs can lead to a novel mechanism for a strongly first-order electroweak phase transition (EWPhT), through their tendency to drive the Higgs quartic coupling negative. These same fermions could also enhance the loop-induced branching fraction of the Higgs into two photons, as suggested by the recent discovery of a ~ 125 GeV Higgs-like state at the CERN Large Hadron Collider (LHC). Our results suggest that measurements of the diphoton decay rate of the Higgs and its self coupling, at the LHC or perhaps at a future lepton collider, could probe the EWPhT in the early Universe, with significant implications for the viability of electroweak baryogenesis scenarios.

The new boson, recently discovered by the CERN Large Hadron Collider (LHC) experiments at 125 GeV [1, 2], has properties very similar to those of the Standard Model (SM) Higgs boson associated with electroweak symmetry breaking (EWSB). While the current data is inconclusive, the measured properties of the new particle, henceforth referred to as the Higgs and denoted by H , seem to show some mild deviations from the SM expectations. In particular, a hint for the deviation in the loop-induced Higgs diphoton decay ($H \rightarrow \gamma\gamma$) rate could be caused by new heavy particles, likely within the reach of the LHC, that couple to the Higgs with $\mathcal{O}(1)$ strength¹. Vector-like fermions, *i.e.* endowed with electroweak preserving masses, are leading candidates [3–6] given that their masses may naturally be around the weak scale. It is interesting to investigate whether these fermions could play a role in addressing some of the open questions in the SM.

In this work we point out that the above vector-like fermions could also lead to a strongly first-order electroweak phase transition (EWPhT) in the early Universe. In typical models of electroweak baryogenesis (EWBG), such a strong phase transition is responsible for the requisite decoupling of baryon number violating processes in the broken phase (with $\langle H \rangle \neq 0$). These baryogenesis scenarios are quite interesting, as they could in principle be directly tested in TeV-scale collider experiments. Our work hence provides a potential connection between the rate for $H \rightarrow \gamma\gamma$ and early Universe cosmology.

The possibility of strengthening the EWPhT through heavy fermions coupled to the Higgs was first considered in Ref. [7], where the authors showed that, contrary to the usual lore, new weak scale bosons are not necessary for that purpose. The mechanism proposed in Ref. [7]

relies on a transfer of entropy from decoupling fermionic degrees of freedom after EWSB. Here, we point out that vector-like fermions can lead to a strongly first-order EWPhT through a combination of a negative quartic coupling (at finite temperature) together with stabilizing higher-dimension operators. Such a mechanism is distinct from those involving new weak scale bosons coupled to the Higgs that lead to cubic terms (e.g. Refs. [10–12]). Instead, the mechanism underlying the phase transition is closely related to that proposed in Ref. [13], and studied in greater detail in Ref. [14]. (For an earlier discussion of the effect of higher dimension operators on EWPhT see Ref. [15].) The vector-like fermion system, that may have a rather interesting connection to the Higgs diphoton rate, can be regarded as a realization of features postulated in Ref. [13]. We will come back to the connection between our setup and other previous works at the end.

To give a simple picture of how the mechanism works, let us first consider a phenomenological description that captures the dominant features. For this purpose, we will ignore the cubic term that can arise from the SM bosonic degrees of freedom and concentrate on the following terms in the 1-loop thermal potential $V(\phi, T)$

$$V(\phi, T) \sim \frac{1}{2}\mu^2\phi^2 + \frac{1}{4}\lambda\phi^4 + \frac{1}{6}\gamma\phi^6, \quad (1)$$

for the background field ϕ associated with the Higgs. All of these terms are temperature-dependent, although we do not indicate it explicitly. We will discuss later a specific model that realizes this scenario with the dimension-6 term being positive. As we will see, the crucial feature is that the quartic coupling λ can become negative at finite temperature. Since at sufficiently high temperature the mass term becomes positive, we will assume a situation where $\mu^2 > 0$, $\lambda < 0$ and $\gamma > 0$. In this case, there is a local minimum at the origin, separated by a barrier from a second minimum at $|\phi| \sim \sqrt{-\lambda/\gamma}$. The associated potential energy contribution from the ϕ^4 and ϕ^6 terms is of order $\lambda^3/(12\gamma^2)$. This minimum becomes degenerate with the minimum at the origin when $\lambda^2 \sim 6\gamma\mu^2$, which will determine the critical temperature through the T -dependence of these parameters. We see that when γ is suppressed by a high mass scale, this occurs when $|\lambda|$ is small, which can happen for relatively

¹ Since the completion of this paper and during the review process, the ATLAS and CMS experiments updated their results on $H \rightarrow \gamma\gamma$. While the ATLAS data mildly favors, at the 2σ level, an enhanced rate for this decay [8], the CMS collaboration now reports a slightly suppressed rate, at the 1σ level [9]. Clearly, more data is needed for a definite conclusion regarding the signal strength for $H \rightarrow \gamma\gamma$.

low temperatures. In addition, we can estimate the vacuum expectation value (vev) at the critical temperature as $\phi_c \sim \sqrt{\mu}/\gamma^{1/4}$, which can be relatively large. This suggests that, provided the conditions above can be realized, the ratio ϕ_c/T_c can be sizeable, and one can expect a strongly first-order EWPhT.

By contrast, when the barrier (and therefore the first-order phase transition) is driven by a cubic term, $ET|\phi|^3$, one has $\phi_c/T_c \sim E/\lambda$, where E is typically small. For instance, in the SM, $E \sim (4\pi\alpha_W^3)^{1/2}$ is far too small since $\sqrt{4\pi\alpha_W}$ is a weak coupling constant. This is one of the reasons why EWBG is widely regarded as requiring physics beyond the SM, so as to enhance the size of E .

The desired features can arise as follows. Consider adding to the SM a single new vector-like fermion pair (χ, χ^c) with a (vector-like) mass m_χ , that couples to the Higgs field via the dimension-5 operator

$$\Delta\mathcal{L} = 2G_m H^\dagger H \chi\chi^c + \text{h.c.} , \quad (2)$$

where G_m is a coefficient with mass dimension -1. It will prove useful to present our results from an effective field theory (EFT) perspective that is, as much as possible, independent of any particular UV completion, although later on we will give a simple UV model that leads to Eq. (2) with $G_m > 0$. We have notationally assumed above that χ is an $SU(2)_L$ singlet since such a new fermion will be subject to relatively mild constraints from EW precision measurements. However, our formalism will apply with trivial modifications when χ is a doublet, with the appropriate contractions with the Higgs fields in Eq. (2).

An immediate consequence of the above operator is that in the presence of a Higgs vev ϕ ($= v = 246$ GeV at zero temperature), the χ mass becomes

$$m_1(\phi) = m_\chi - G_m \phi^2 . \quad (3)$$

We will be interested in the 1-loop effective potential for ϕ , which will receive a contribution from χ through $m_1(\phi)$. In addition, the interaction in Eq. (2) induces divergences in the Higgs sector corresponding to “tree-level” operators

$$V_0(\phi) = V_{\text{tree}} + \frac{1}{6}\bar{\gamma}\phi^6 + \frac{1}{8}\bar{\delta}\phi^8 , \quad (4)$$

where $\bar{\gamma}$ and $\bar{\delta}$ are free parameters from an EFT point of view (the bars indicate that we will be thinking of them as being defined in the $\overline{\text{MS}}$ scheme). We have denoted by V_{tree} the usual quadratic and quartic Higgs terms. In preparation for the analysis of the high-temperature properties, it is convenient to impose on the effective potential the conditions $V'(v) = 0$ and $V''(v) = m_H^2$ at $T = 0$, where v and m_H are the Higgs vev and mass, respectively [16]. This trades the squared mass parameter and Higgs quartic coupling in V_{tree} for v and m_H , while

fixing the 1-loop contribution due to the new fermion to

$$V_1(\phi) = -\frac{4}{64\pi^2} m_1^4(\phi) \text{Ln}(m_1^2(\phi)) + \frac{1}{2}\alpha(m_1^2(v))\phi^2 + \frac{1}{4}\beta(m_1^2(v))\phi^4 , \quad (5)$$

where $\text{Ln}(\omega) \equiv \ln(\omega/\mu^2) - \frac{3}{2}$, with μ the renormalization scale, and

$$\alpha(\omega) = -\frac{4}{64\pi^2} \left\{ \left(-3\frac{\omega\omega'}{v} + \omega'^2 + \omega\omega'' \right) \text{Ln}(\omega) - \frac{3}{2} \left(\frac{\omega\omega'}{v} - \omega'^2 - \frac{1}{3}\omega\omega'' \right) \right\} + \bar{\gamma}v^4 + 2\bar{\delta}v^6 , \quad (6)$$

$$\beta(\omega) = -\frac{4}{128\pi^2 v^2} \left\{ 2 \left(\frac{\omega\omega'}{v} - \omega'^2 - \omega\omega'' \right) \text{Ln}(\omega) + \left(\frac{\omega\omega'}{v} - 3\omega'^2 - \omega\omega'' \right) \right\} - 2\bar{\gamma}v^2 - 3\bar{\delta}v^4 . \quad (7)$$

This generalizes the expressions derived in Ref. [7] to the non-renormalizable case that involves the new parameters $\bar{\gamma}$ and $\bar{\delta}$, with the explicit factor of 4 counting the new fermionic degrees of freedom.

Adding the temperature-dependent contributions (for a discussion of the relevant formalism see for example Ref. [17]), the free energy reads

$$\mathcal{F} = V(\phi) + \mathcal{F}_1(\phi, T) , \quad (8)$$

where $V(\phi) = V_0(\phi) + V_1(\phi)$ is the zero-temperature potential discussed above, now including the well-known SM contributions from the top quark and weak gauge bosons.² The 1-loop thermal function \mathcal{F}_1 is given by

$$\mathcal{F}_1(\phi, T) = \sum_i \frac{g_i T^4}{2\pi^2} I_{\mp} \left(\frac{m_i(\phi)}{T} \right) , \quad (9)$$

with $I_{\mp}(z) = \pm \int_0^\infty dx x^2 \ln(1 \mp e^{-\sqrt{x^2+z^2}})$. The index i runs over all the particles, with number of degrees of freedom given by g_i , whose masses $m_i(\phi)$ depend on ϕ ; the upper and lower signs correspond to bosons and fermions, respectively.

When the new fermion is at the EW scale, it may be appropriate to use the high-temperature expansion of Eq. (9), thus resulting in a potential, presented in the appendix, that is polynomial in ϕ with T -dependent coefficients. However, for the numerical analysis we will

² Although not included in Fig. 1 below, the 125 GeV Higgs gives a subdominant effect in the regions of interest. We note here, however, that the Higgs slightly strengthens the EWPhT by lowering T_c . This conclusion is based on the formalism of Ref. [18], which uses as a source the operator $JH^\dagger H$ instead of the usual linear coupling $JH + \text{h.c.}$. This leads to a *real* 1-loop potential *everywhere*, while maintaining the desired features of the standard effective potential. Also, the Nambu-Goldstone bosons from EWSB do not contribute to the potential.

use the full 1-loop thermal effective potential. The important point, as can be seen in the high-temperature expansion, is that, due to logarithmic terms associated with the fermionic sector of the model, the effective Higgs quartic coupling can become negative at a certain temperature, thus creating a “runaway” behavior that is stabilized by the higher-dimension operators.³ This realizes the basic idea explained in the introduction. It also makes it manifest that the details of the phase transition are UV dependent, since the higher-dimension operators in the Higgs potential are crucial and depend on the undetermined $\bar{\gamma}$ and $\bar{\delta}$. In order to show that a strong phase transition can indeed be realized, we turn to a simple UV model that serves as a “proof of existence.”

The model we will focus on introduces the following new fields (using the notation of Ref. [6], but see also [5])

$$(\psi, \psi^c) \sim (1, 2)_{\pm\frac{1}{2}}, \quad (\chi, \chi^c) \sim (1, 1)_{\mp 1}, \quad (10)$$

where the charges correspond to the SM $SU(3) \times SU(2) \times U(1)_Y$ quantum numbers. These charges allow the following mass terms for the new fermions

$$-\mathcal{L}_m = m_\psi \psi \psi^c + m_\chi \chi \chi^c + y H \psi \chi + y_c H^\dagger \psi^c \chi^c + \text{h.c.} \quad (11)$$

In the following we will assume, for simplicity, that $y = y_c$, in which case we have two mass eigenstates with electric charges $|Q_i| = 1$ and squared masses given by

$$\begin{aligned} m_{1,2}^2(\phi) &= \frac{1}{2} (m_\psi^2 + m_\chi^2) + \frac{1}{2} y^2 \phi^2 \\ &\mp \frac{1}{2} (m_\psi + m_\chi) \sqrt{(m_\psi - m_\chi)^2 + 2y^2 \phi^2}. \end{aligned} \quad (12)$$

The spectrum also contains a neutral state N with mass $m_N = m_\psi$.

We will consider the above model in the limit where $m_\psi \gg yv$ (while m_χ is at the EW scale). In this limit, it is appropriate to integrate out the heavy state with mass of order $m_2(\phi) \approx m_\psi$, which can then be seen to generate the operator in Eq. (2) with

$$G_m = \frac{Z_m y^2}{2(m_\psi - m_\chi)}. \quad (13)$$

At tree-level one finds $Z_m = 1$ and one can check that Eq. (2) reproduces $m_1(\phi)$ in Eq. (12) to order ϕ^2 . We allow for a non-trivial factor Z_m to investigate the possible impact of higher-order loop corrections at the matching scale, since we will later be interested in a region where the Yukawa coupling, y , is sizeable. The model also predicts that $\bar{\gamma} = \bar{\gamma}_{\text{th}} + \bar{\gamma}_{\text{RG}}$ and $\bar{\delta} = \bar{\delta}_{\text{th}} + \bar{\delta}_{\text{RG}}$ (see the

³ In some examples the Higgs quartic at T_c is positive but sufficiently small to allow for the SM cubic term to induce the desired “runaway” behavior.

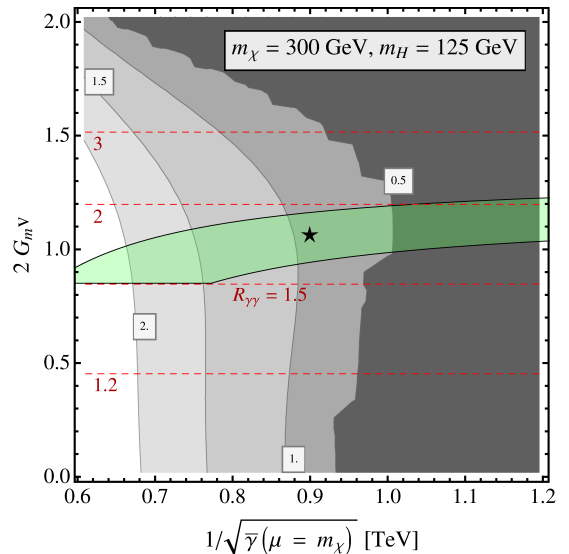


FIG. 1: Contours of constant ϕ_c/T_c in the EFT (gray) defined by Eqs. (4)-(9), together with the diphoton enhancement (dashed red horizontal lines). The star corresponds to the benchmark point in the UV model, while the light green region (narrow horizontal band) corresponds to a 20% variation in Z_m and Z_γ in that benchmark. Up to a sign, the vertical axis is the effective Yukawa coupling of the light fermion to the Higgs (see text).

appendix), where

$$\bar{\gamma}_{\text{th}} = \frac{Z_\gamma y^6}{16\pi^2} \frac{m_\psi (m_\psi^2 + 7m_\chi m_\psi - 2m_\chi^2)}{(m_\psi - m_\chi)^5}, \quad (14)$$

$$\bar{\delta}_{\text{th}} = -\frac{Z_\delta y^8}{48\pi^2} \frac{7m_\psi^3 + 27m_\chi m_\psi^2 - 4m_\chi^3}{(m_\psi - m_\chi)^7}, \quad (15)$$

are the threshold contributions induced at $\mu = m_\psi$, and

$$\bar{\gamma}_{\text{RG}} \approx -\frac{3G_m^3 m_\chi}{2\pi^2} \ln \left(\frac{m_\psi^2}{\mu^2} \right), \quad (16)$$

$$\bar{\delta}_{\text{RG}} \approx \frac{G_m^4}{2\pi^2} \ln \left(\frac{m_\psi^2}{\mu^2} \right), \quad (17)$$

are the running contributions between m_ψ and a lower scale μ . Here, we parametrized possible higher-order loop effects at the matching scale through the factors Z_γ and Z_δ (at lowest order, $Z_\gamma = Z_\delta = 1$).

In Fig. 1, we show the contours of ϕ_c/T_c in the plane of $G_m v$ versus (the low-energy) $\sqrt{1/\bar{\gamma}}$, in a model-independent analysis based on Eqs. (4)-(9), fixing $m_\chi = 300$ GeV. We also indicate with a star a benchmark point corresponding to the UV model discussed above [i.e. using Eqs. (13)-(17)]. This benchmark has $m_\chi = 300$ GeV, $m_\psi = 4$ TeV and $y = 4$. For $Z_m = Z_\gamma = Z_\delta = 1$, one has $m_1(v) \approx 170$ GeV (satisfying a naive LEP 2 bound of ~ 100 GeV), and the phase transition occurs at a critical temperature $T_c \approx 150$ GeV when $\phi_c \approx 140$ GeV so

that $\phi_c/T_c \approx 0.93$.⁴ When the Higgs contributions are included, we find $\phi_c/T_c \approx 1.1$. Note also that at $\phi = \phi_c$ the light fermion has a mass $m_1(\phi_c) \approx 260$ GeV and is heavier than at $T = 0$, which is an effect opposite to the case considered in Ref. [7].

The first-order phase transition arises as described in the introduction, relying on a negative quartic coupling at finite temperature, stabilized by the dimension-6 operator in Eq. (4). The mechanism depends mainly on the fermion contributions (both χ and the top quark). In particular, even if the contributions from the W and Z are ignored we still find a strongly first-order phase transition. Thus, unlike other scenarios, a term cubic in ϕ need not play a crucial role.⁵ We note that at very small $G_m v$, one recovers the scenario discussed in [13], as seen from Eq. (7) when the light fermion contributions are decoupled and the negative contribution to the quartic due to β is dominated by the (positive) $\bar{\gamma}$ term. We also note that for values of $\bar{\gamma}$ larger than exhibited in the figure, a minimum at the origin may develop even at $T = 0$, in which case one should make sure that the EWSB minimum is the global one [13]. In this region, however, the EFT may not give an accurate description of the physics, so we explicitly exclude it.

We have also checked in selected examples the efficiency with which the nucleation process takes place by computing numerically the bounce action, $S_E(T)$, and checking that $B(T_n) \equiv S_E(T_n)/T_n$ can reach the desired range $130 \lesssim B(T_n) \lesssim 140$, for nucleation temperatures T_n around 100 GeV even when the phase transition is sufficiently strong to allow for EWBG. When ϕ_c/T_c becomes too large, however, the nucleation rate becomes exponentially suppressed. This will limit, but not exclude, phenomenologically interesting regions with a strongly first-order phase transition.

As illustrated by the benchmark example, within the UV model, a sizeable underlying Yukawa coupling is required.⁶ Hence, we also show in the figure a contour around the previous benchmark point exhibiting the result of varying Z_m and Z_γ within 20% to provide a feel

for the sensitivity to the higher-order loop effects at the matching scale m_ψ . We see that there is a significant sensitivity of ϕ_c/T_c , especially to Z_γ which is responsible for the horizontal variation in the plot, as it affects the coefficient of the stabilizing dimension-6 operator.

We also note that after EWSB the operator in Eq. (2) induces an effective Yukawa coupling between the new fermion and the Higgs boson given by $y_{\text{eff}} = -2G_m v$. The requirement of a strongly first-order phase transition implies that this Yukawa coupling be of order one. Thus, we can expect a relevant modification of the Higgs branching fractions, in particular the $H \rightarrow \gamma\gamma$ rate when χ is electrically charged. Interestingly, the fact that G_m is positive means that the new fermion mass decreases as the Higgs vev increases, which implies an enhancement of the diphoton rate [4]. In the presence of a charged vector-like fermion, the ratio of the branching fraction into the diphoton final state to its SM value is given by

$$R_{\gamma\gamma} \simeq \left| 1 - \frac{F_{1/2}(\tau_1) Q_1^2}{F_{\text{SM}}} \frac{\partial \ln m_1(v)}{\partial \ln v} \right|^2, \quad (18)$$

where $F_{\text{SM}} \simeq -6.49$ is associated with the SM amplitude, $\tau_1 = 4m_1^2/m_H^2$, and $F_{1/2}(\tau)$ is the familiar loop function (see e.g. Ref. [20]). In Fig. 1, we have also superimposed the lines of constant $R_{\gamma\gamma}$ (dashed-red lines). As one can see, the region with a strongly first-order phase transition corresponds to values of $R_{\gamma\gamma} > 1$ in the vicinity of the benchmark point.

Also, the dimension-6 operator of Eq. (4) affects the Higgs boson triple coupling $V'''(v) = 3m_H^2/v + 8\bar{\gamma}v^3$, where Eq. (4) is used, ignoring the ϕ^8 operator; the first term is the usual SM contribution. As discussed previously and shown in Fig. 1, for a first order EWPhT a positive $\bar{\gamma} \sim (1 \text{ TeV})^{-2}$ is required. This corresponds to increasing the SM prediction of the triple Higgs coupling by $\mathcal{O}(1)$. Naively, this increase in the Higgs triple coupling would indicate an increased signal rate for $gg \rightarrow HH$ at the LHC. However, Higgs pair production proceeds through destructively interfering top quark box and off-shell s -channel Higgs boson amplitudes, with the box diagram being the dominant contribution. Hence, a moderate increase in the Higgs triple coupling increases the s -channel Higgs contribution and paradoxically decreases the LHC Higgs pair production rate. For $(600 \text{ GeV})^{-2} \gtrsim \bar{\gamma} \gtrsim (900 \text{ GeV})^{-2}$, the pair production rate is expected to be 40 – 60% of the SM prediction at the LHC. With full SM strength, it is estimated to take around several ab^{-1} of data at the 14 TeV LHC to exclude a $V'''(v) = 0$ at 90% CL [21], making this measurement very challenging at the LHC. However, with 2 ab^{-1} of data, a 500 GeV and 1 TeV ILC are expected to measure the Higgs self-coupling with an accuracy of $\sim 44\%$ and $\sim 17\%$ respectively [22]. Hence, with a sufficient amount of data, the ILC can examine one of the key implications of this EWPhT scenario. In addition, a measurement of the light fermion mass m_1 and the diphoton rate could be used to infer m_χ and $G_m v$ within the framework. This, together with some

⁴ We note that the same qualitative features can be obtained by a naive application of the Coleman-Weinberg potential to the full theory defined by Eqs. (10) and (11) [for the benchmark point one finds $\phi_c \approx 128$ GeV and $T_c \approx 146$ GeV, so that $\phi_c/T_c \approx 0.88$]. However, the EFT analysis clarifies the origin of the strongly first-order EWPhT, allows us to understand the large logarithms, and permits a simple estimate of the higher-order loop effects at the matching scale.

⁵ We do not include the “daisy resummation” [19] which would somewhat affect the cubic terms from the SM, but we expect its impact to be relatively minor.

⁶ We also found regions of parameter space, within the UV model of Eq. (11), with $y \sim 2.5$ and roughly degenerate m_χ and m_ψ of order a few hundred GeV (with the same sign), where one could achieve a strongly first-order phase transition for $m_1 \gtrsim 100$ GeV. However, such regions of parameter space give rise to suppression of the Higgs diphoton rate, which is disfavored by the current data from the LHC.

knowledge about $\bar{\gamma}$ from the Higgs boson triple coupling could identify the relevant region in Fig. 1, and start giving information regarding the nature of the phase transition and its strength. (For earlier work on the possible connection between Higgs self-coupling and EWPhT see Ref. [23])

The model in Eq. (10) does not allow for the decay of the light charged fermion. To avoid this situation (which could lead to severe bounds on m_1), we could either assume that (ψ, χ) mix with the SM leptons or else postulate another heavy vector-like lepton n with no SM charges [6]. In the latter case, additional terms of the form $H\psi n$ result in the appearance of two neutral states, $n_{1,2}$, where n_1 could be lighter than χ and lead to $\chi \rightarrow n_1 W$ (W on- or off-shell). The new neutral states can enhance the strength of the EWPhT, without affecting $R_{\gamma\gamma}$.

A second comment refers to a potential instability of the $T = 0$ EFT potential at large field values. Using the SM RG equations together with the contributions to the β -function discussed in the appendix, and using for illustration the point marked by a star in the figure, one can check that the Higgs quartic coupling becomes negative at a scale of about 700 GeV. However, this regime is outside the range of validity of the EFT analysis, and higher powers of ϕ can play a crucial role. In fact, a naive application of the Coleman-Weinberg potential to the full UV model suggests that when the infinite tower of operators is resummed the instability is pushed to about 3.5 TeV. Although new (bosonic) degrees of freedom would likely be required at this scale, they need not affect the physics of the EWPhT or the diphoton rate.

Given the sizable Yukawa couplings at the scale $m_\psi = 4$ TeV, one may generically expect the emergence of new strong dynamics and a composite Higgs at a scale $\Lambda_c > m_\psi$. In principle, the addition of singlet scalars S with masses $m_S \sim 1$ TeV and couplings to the Higgs of the same order as the vector fermion Yukawas, say through a term $S^2 H^\dagger H$, could delay the instability sufficiently above m_ψ , so that our UV model can be a valid effective description for a reasonable choice of $\Lambda_c > m_\psi$. Above Λ_c , the Higgs is no longer a fundamental degree of freedom and the problem of instability can be resolved. The most promising LHC signature of these additional states would likely be associated with the lightest scalar, S_0 . In this simple setup, after EWSB, we expect that S_0 can be pair produced through s -channel Higgs intermediate states. If S_0 is stable on collider time scales, extra initial state radiation may be necessary in order to detect a sizable missing p_T signal, for example in vector boson fusion, using hard forward tagging jets [24]. However, if S_0 can develop a vev, it can be singly produced by mixing with the Higgs and eventually decay into a Higgs pair. Such events will give rise to 4- b -jet final states. A detailed discussion of the prospects for detecting such signals are beyond the scope of this paper (however, for some recent work in this direction see Ref. [25]).

Finally, we would like to comment on the connection

to previous works that share some elements of our setup and discussion. Ref. [13] has examined the effects on the EWPhT caused by higher dimension operators in the Higgs potential (see also Refs. [14, 26] for further work in this direction). In particular, they considered how a *zero-temperature* negative quartic could be stabilized by a dimension-6 operator in their setup. While this is a qualitative feature also observed in our mechanism, we point out that in our model the negative quartic is induced by the new fermion (with some help from the top quark) at high temperatures and is not a feature of the $T = 0$ potential. In fact, the analysis of Ref. [13] ignored thermally induced quartic terms, although they were fully included in Ref. [14]. Without the new fermionic contribution, the cubic term from the SM would still play an essential role.

As mentioned in the introduction, Ref. [7] has also studied how new heavy fermions with large couplings to the Higgs can lead to an enhanced first order phase transition. The mechanism studied in Ref. [7] is mainly based on transfer of entropy as the new fermions get *heavier* and decouple from the plasma after EWSB. We note that our results do not rely on this thermodynamic effect since the relevant weak scale fermion in our mechanism gets *lighter* and remains active in the thermal bath after EWSB. Note also that this feature, i.e. the decrease in the fermion mass as ϕ increases, is the reason that our mechanism also leads to an enhancement in the diphoton branching fraction of the Higgs, while the fermion couplings in Ref. [7] would lead to a suppression.

To conclude, we have shown that the tendency of fermions, that couple with $\mathcal{O}(1)$ strength to the Higgs, to drive the Higgs quartic coupling negative can be related to a strongly first-order EWPhT. We provided a concrete realization where the Higgs potential is stabilized by higher-dimension operators that arise from a system of heavy and light vector-like fermion pairs. We note that the main ingredients (one fermion with mass in the multi-TeV scale, a second fermion parametrically lighter, and a semi-perturbative underlying Yukawa interaction) can naturally arise in scenarios based on a warped extra dimension. This can potentially establish a connection between our observation and the physics of EWSB, as well as the solution to the hierarchy problem. Furthermore, the same fermions can also enhance the rate for $H \rightarrow \gamma\gamma$, as may be suggested by the early LHC data. As noted earlier, the current status of the experimental results does not offer a clear picture regarding the signal strength for $H \rightarrow \gamma\gamma$, with the ATLAS experiment reporting a modest enhancement and the CMS results yielding a mild suppression compared to the SM expectation. We find that the Higgs diphoton decay rate and the strength of the EWPhT can be correlated, as shown in the simple model above. Also, a typical consequence of our setup is an enhancement of the triple Higgs boson coupling that could be probed at the LHC or, more likely, at a future lepton collider.

In this appendix, we derive the effective theory at 1-

loop order, valid below the heavy fermion mass $m_2 \approx m_\psi$ in the model defined by Eqs. (10) and (11). We work in the $\overline{\text{MS}}$ scheme, matching the ϕ correlators up to 8th order. In the UV theory, which describes both fermionic states, ψ and χ , the correlators can be read from the Coleman-Weinberg potential in the $\overline{\text{MS}}$ scheme

$$V_{\text{UV}} = V_{\text{tree}} - \frac{4}{64\pi^2} \sum_{i=1,2} m_i^4(\phi) \left[\ln \left(\frac{m_i^2(\phi)}{\mu^2} \right) - \frac{3}{2} \right],$$

where the m_i are given in Eq. (12). Similarly, the correlators in the effective theory are read from

$$V_{\text{EFT}} = V_0 - \frac{4m_1^4(\phi)}{64\pi^2} \left[\ln \left(\frac{m_1^2(\phi)}{\mu^2} \right) - \frac{3}{2} \right], \quad (\text{A.19})$$

where V_0 is defined in Eq. (4), and we include only the light state, with a mass given in Eq. (12). Comparing the ϕ^6 and ϕ^8 terms in both theories, and requiring that they agree at $\mu = m_\psi$, fixes the corresponding threshold corrections as given in Eq. (14) and (15). The matching contributions to the mass parameter and Higgs quartic are not interesting since they will be traded for v and m_H . However, the running of all the parameters below m_ψ is of interest. The β -functions can be derived from the requirement that the effective potential in Eq. (A.19) be RG invariant:

$$\sum_a \left(\beta_a \frac{\partial}{\partial \lambda_a} - \gamma_\phi \phi \frac{\partial}{\partial \phi} \right) V_0 = -\frac{4}{32\pi^2} m_1^4(\phi),$$

where γ_ϕ is the ϕ anomalous dimension, and we may use $m_1(\phi) = m_\chi - G_m \phi^2$, which corresponds to keeping only the operator (2) in the EFT. Noting that this operator does not induce any wavefunction renormalization for ϕ at one loop, this leads to the β -functions in the $\overline{\text{MS}}$ scheme:

$$\Delta\beta_\lambda = -\frac{3G_m^2 m_\chi^2}{\pi^2}, \quad \beta_\gamma = \frac{3G_m^3 m_\chi}{\pi^2}, \quad \beta_\delta = -\frac{G_m^4}{\pi^2}.$$

The operator in Eq. (2) renormalizes both m_ψ and G_m itself. However, the first effect vanishes in the EW symmetry preserving limit (when the Higgs is massless), while the second effect is of second order in the small quantity G_m , thus leading to a rather mild μ -dependence. Neglecting these effects, as well as the renormalization due to the weak interactions, the RG equations can be solved immediately to produce Eqs. (16) and (17).

We also provide the effective potential in the EFT using the high-temperature expansion and neglecting the weak gauge boson contributions. Note that the heavy fermion state will be efficiently Boltzmann suppressed at

temperatures relevant to EWPhT and hence it can be ignored. Up to a constant term,

$$V(\phi) = \frac{1}{2} \mu_{\text{eff}}^2 \phi^2 + \frac{1}{4} \lambda_{\text{eff}} \phi^4 + \frac{1}{6} \gamma_{\text{eff}} \phi^6 + \frac{1}{8} \delta_{\text{eff}} \phi^8 + \mathcal{O}(\phi^{10}),$$

where

$$\begin{aligned} \mu_{\text{eff}}^2 &= -\frac{m_H^2}{2} + \frac{T^2}{12} (3y_t^2 - 4G_m m_\chi) - \frac{3y_t^4 v^2}{16\pi^2} \\ &\quad + \alpha + \frac{G_m m_\chi^3}{2\pi^2} \ln \left(\frac{A_F T^2}{\mu^2} \right), \\ \lambda_{\text{eff}} &= \frac{m_H^2}{2v^2} + \beta - \frac{3y_t^4}{16\pi^2} \ln \left(\frac{2A_F T^2}{y_t^2 v^2} \right) \\ &\quad + \frac{1}{3} G_m^2 T^2 - \frac{3G_m^2 m_\chi^2}{2\pi^2} \ln \left(\frac{A_F T^2}{\mu^2} \right), \\ \gamma_{\text{eff}} &= \bar{\gamma} + \frac{3G_m^3 m_\chi}{2\pi^2} \ln \left(\frac{A_F T^2}{\mu^2} \right), \\ \delta_{\text{eff}} &= \bar{\delta} - \frac{G_m^4}{2\pi^2} \ln \left(\frac{A_F T^2}{\mu^2} \right). \end{aligned}$$

$\alpha = \alpha(m_1^2(v))$ and $\beta = \beta(m_1^2(v))$ are defined in Eqs. (6) and (7) [by definition, these include only the new light fermion field], $\bar{\gamma}$ and $\bar{\delta}$ are defined by Eq. (4), and $A_F = \pi^2 e^{-2\gamma_E}$ with γ_E the Euler-Mascheroni constant. We emphasize that the above expression is independent of the UV completion. One can check that the explicit μ -dependence cancels out when Eqs. (16) and (17) are used. Note also that the contribution to the thermal mass from the light fermion state is negative. However, even in the absence of the top quark, at sufficiently high temperatures, the heavy fermion (or more generally the heavy states in the UV completion) gives a positive contribution to the thermal mass that restores the EW symmetry, as expected. Thus, the above potential has a region of validity in temperature with both upper and lower bounds. For temperatures of order the EW scale it should provide an appropriate description of EWPhT.

Acknowledgments

We thank D. Marzocca, M. Serone and A. Urbano for pointing out an error in a previous version of this work. This led us to consider a different region of parameter space, where the original conclusions could be obtained. We also thank Mariano Quirós for comments on the revised manuscript, and Sally Dawson for helpful conversations. This work is supported by the US Department of Energy under Grant Contract DE-AC02-98CH10886.

[1] G. Aad *et al.* [ATLAS Collaboration], Phys. Lett. B **716**, 1 (2012) [arXiv:1207.7214 [hep-ex]].

[2] S. Chatrchyan *et al.* [CMS Collaboration], Phys. Lett. B **716**, 30 (2012) [arXiv:1207.7235 [hep-ex]].

- [3] S. Dawson and E. Furlan, Phys. Rev. D **86**, 015021 (2012) [arXiv:1205.4733 [hep-ph]]; N. Bonne and G. Moreau, arXiv:1206.3360 [hep-ph]; H. An, T. Liu and L. -T. Wang, arXiv:1207.2473 [hep-ph]. A. Joglekar, P. Schwaller and C. E. M. Wagner, arXiv:1207.4235 [hep-ph]. H. Davoudiasl, H. -S. Lee and W. J. Marciano, arXiv:1208.2973 [hep-ph];
- [4] M. Carena, I. Low and C. E. M. Wagner, JHEP **1208**, 060 (2012) [arXiv:1206.1082 [hep-ph]].
- [5] L. G. Almeida, E. Bertuzzo, P. A. N. Machado and R. Z. Funchal, arXiv:1207.5254 [hep-ph]; J. Kearney, A. Pierce and N. Weiner, arXiv:1207.7062 [hep-ph]; M. B. Voloshin, arXiv:1208.4303 [hep-ph];
- [6] N. Arkani-Hamed, K. Blum, R. T. D’Agnolo and J. Fan, arXiv:1207.4482 [hep-ph].
- [7] M. S. Carena, A. Megevand, M. Quirós and C. E. M. Wagner, Nucl. Phys. B **716**, 319 (2005) [hep-ph/0410352];
- [8] “Latest ATLAS studies on Higgs to diboson states,” talk by Fabrice Hubaut at Rencontres de Moriond 2013, EW session, March 2-9.
- [9] “Study of Higgs Production in Bosonic Decay Channels at CMS,” talk by Christophe Ochando at Rencontres de Moriond 2013, QCD session, March 9-16.
- [10] J. R. Espinosa, M. Quirós and F. Zwirner, Phys. Lett. B **307**, 106 (1993) [hep-ph/9303317].
- [11] M. S. Carena, M. Quirós and C. E. M. Wagner, Phys. Lett. B **380**, 81 (1996) [hep-ph/9603420].
- [12] For recent work that explores the connection between the EWPhT and the $H \rightarrow \gamma\gamma$ rate, invoking extra bosonic degrees of freedom, see D. J. H. Chung, A. J. Long and L. -T. Wang, arXiv:1209.1819 [hep-ph], and W. Huang, J. Shu and Y. Zhang, arXiv:1210.0906 [hep-ph].
- [13] C. Grojean, G. Servant and J. D. Wells, Phys. Rev. D **71**, 036001 (2005) [hep-ph/0407019].
- [14] C. Delaunay, C. Grojean and J. D. Wells, JHEP **0804**, 029 (2008) [arXiv:0711.2511 [hep-ph]].
- [15] X. -m. Zhang, Phys. Rev. D **47**, 3065 (1993) [hep-ph/9301277].
- [16] G. W. Anderson and L. J. Hall, Phys. Rev. D **45**, 2685 (1992).
- [17] M. Quirós, hep-ph/9901312.
- [18] K. E. Cahill, Phys. Rev. D **52**, 4704 (1995) [hep-ph/9301294].
- [19] L. Dolan and R. Jackiw, Phys. Rev. D **9**, 3320 (1974).
- [20] J. F. Gunion, H. E. Haber, G. Kane and S. Dawson, *The Higgs Hunter’s Guide*, Addison Wesley Publishing Company (1990).
- [21] U. Baur, T. Plehn and D. L. Rainwater, Phys. Rev. D **69**, 053004 (2004) [hep-ph/0310056]; K. Jakobs, Eur. Phys. J. C **59**, 463 (2009).
- [22] H. Baer et al., *ILC DBD*, Physics at the International Linear Collider, to be published in the ILC Detailed Baseline Design Report.
- [23] A. Noble and M. Perelstein, Phys. Rev. D **78**, 063518 (2008) [arXiv:0711.3018 [hep-ph]].
- [24] H. Davoudiasl, R. Kitano, T. Li and H. Murayama, Phys. Lett. B **609**, 117 (2005) [hep-ph/0405097].
- [25] M. Gouzevitch, A. Oliveira, J. Rojo, R. Rosenfeld, G. Salam and V. Sanz, arXiv:1303.6636 [hep-ph].
- [26] D. Bodeker, L. Fromme, S. J. Huber and M. Seniuch, JHEP **0502**, 026 (2005) [hep-ph/0412366].